

## RESPONSE OF CYLINDRICAL ELEVATED WHEAT STORAGE SILOS TO SEISMIC LOADING

Hamdy H. A. Abdel-Rahim

Associate Professor, Civil Eng. Department, Faculty of Engineering, Assiut University

Received 28 October 2013; accepted 30 November 2013

### ABSTRACT

The elevated cylindrical storage silos are lifeline structures and strategically very important, since they have vital use in industries. Silos are special structures subjected to many different unconventional loading conditions, which result in unusual failure modes. In addition silos are cantilever structures with the material stacked up very high vertically. The earthquake response of silo structures for the storage of bulk solids differs for elevated silos and silos supported directly on the ground. The walls of different type of silos are subject to earthquake loads from the stored mass, and these may substantially exceed the pressures from filling and discharge. The assessment of horizontal action of ensiled material due to seismic vent seems to be particular interest. This paper is concerned with the earthquake response of these structures, which has received little attention to date. A cylindrical silo wall and bulk solid is modeled by three dimensional finite solid elements. The interaction effect between the silo wall and bulk solid is taking account by using the nonlinear approach proposed by Duncan and Chang [5]. A then interface layer proposed by Desia [4] is applied to describe the phenomena taking place on the surface between the granular material and silo wall. Coulomb's friction law was used for modeling of wall friction. An incremental iterative finite element technique is applied for dynamic analysis of wheat silos using SAP2000 structural software package [3]. In this research seven reinforced concrete silo models with different height to diameter ratios were studied and analyzed in time history by using earthquake acceleration 0.5g applied to silos models. The resulting finite element silo pressures as the silo is full with and without earthquake excitation are compared with theoretical filling and discharging pressure. The result obtained revealed that the elevated silos response is highly influenced by the earthquake characteristics and is depending on the height to diameter ratio. Also the findings indicate that the squat silos (large diameter to height ratio) are more resistance to the earthquake and more economical. The seismic responses of the elevated wheat silo such as top displacement, normal forces, shearing forces and bending moments in silo support have been assessed for earthquake records.

**Keywords:** Seismic behaviour, Bulk and granular solids, Time history analysis, Filling, Discharging, Wheat silos

### 1. Introduction

There are three principal methods of calculating silos—(i) analytical methods, which incur enormous difficulty in their solution; (ii) experimental methods, of great interest, but also of great cost and influenced by factors of scale; and (iii) numerical methods, of less cost and which have been of great utility and widespread application in the last few decades. Of the numerical methods, there stand out for their importance the finite element method (FEM). One of the difficulties in numerical simulations is simulating the stored granular material. The perspective of the FEM is to view the granular material as a

continuum. These limits its application to silos with stored materials of very large, and not very realistic, particle sizes. Hence, in problems that demand analysis using eight-dimensional models, the FEM would seem to be the most suitable.

Containers used for storing bulk solids are usually called bins, bunkers, silos, or tanks. Although there is no generally accepted definition for these terms, shallow structures containing coal, coke, ore, crushed stone, gravel, and similar materials are often called bins or bunkers, and tall structures containing materials such as grain and cement are usually called silos (Li 1994) [12].

A number of representative silos that were damaged or collapsed during recent earthquakes around the world will be presented in this section. Possible causes of failures and potential measures to prevent damage will be discussed. Earthquakes frequently cause damage and/or collapse in silos resulting in not only significant financial loss but also loss of life. For example, during the 2001 El Salvador earthquake three people lost their lives as a result of a silo failure (Mendez 2001) [14].

An earthquake ground motion has three components resulting in structural loads in the vertical and two horizontal directions. The effect of vertical seismic loads on the relatively heavy silo structures is usually small, whereas the effect of lateral loads can be significant especially on the taller silos containing heavier material. The magnitude of the horizontal seismic load is directly proportional to the weight of the silo. As the silo height increases the height of the center of mass of the silo structure also increases. Assuming the horizontal seismic load is applied roughly at the center of mass, the moment arm for the lateral load and the corresponding bending moment at the base increase. The increased bending moment then results in non-uniform pressure distribution at the bottom of the silo, which can be significantly larger than the pressure caused by the gravity loads. Earthquakes can also cause damage in the upper portion of the silo if the material contained can oscillate inside the silo during the earthquake. The lateral loads due to material flow and lateral seismic loads must be considered simultaneously if the material can oscillate. Wall pressure is a key parameter to silos' design. It has an important effect on the safety and efficiency of silos. Bulk solids are composed by individual solid particles inside a continuous phase, usually gaseous. The interaction among these particles and the continuous phase is complex, being very difficult to formulate a complete and accurate theoretical description of this problem.

This behaviour is a kind of combination between liquids and solids. A liquid under static conditions cannot transmit shear forces so its pressure increases linearly with depth, independent of the direction. Bulk solids, on the contrary, can form surfaces up to a certain slope, corresponding to the natural angle of frictional stability. They are able to transmit static shear forces and the pressures on the silo wall do not increase linearly with depth, but they quickly reach a maximum, due to the wall friction forces.

### **October 3, 1974 Lima, Peru Earthquake**

The 8.1 magnitude earthquake occurred 80 km southwest of Lima. The tremor killed 78 and injured several thousand people. During this earthquake, a large grain elevator in the port area of Callao lost its head house which fell from the tops of the silos and embedded itself in the adjoining pier. It was reported that this elevator suffered damage earlier in the 1970 Peru earthquake and was considered unsafe (Moran et al. 1975) [15]. This is a good

example of silo damage resulting from failure of a secondary structure or machinery improperly attached to the silo structure.

### **March 2, 1987 Edgecumbe, New Zealand Earthquake**

The earthquake that struck Edgecumbe, New Zealand on March 2, 1987 had a magnitude of 6.1 and a focal depth of 6 km. This was one of the strongest and most damaging earthquakes to hit New Zealand in recent history. At Bay Milk Products facility in Edgecumbe, huge stainless steel milk silos collapsed, spilling thousands of liters of milk. Two milk storage tanks were thrown on their sides.

### **December 7, 1988 Spitak, Armenia Earthquake**

On December 7, 1988, at 11:41 a.m. local time, a magnitude 6.9 earthquake shook northwestern Armenia. Fig. 13 shows the east end of the granary in the flour mill complex east of Spitak. Grain can be seen spilling out of the collapsed concrete shear-wall structures in the foreground. In the background are cast-in-place concrete grain silos. Most such silos had no or only minor damage during the earthquake. However, overall losses at the flour mill complex were large (NGDC 1988) [17]. It should be noted the silo structure that failed during this earthquake was noncylindrical, however its height was comparable to that of the nearby undamaged cylindrical silos.

### **August 17, 1999 Kocaeli and November 12, 1999 Duzce, Turkey Earthquakes**

The 7.4 magnitude Kocaeli and 7.2 magnitude Duzce earthquakes occurred in northwestern Turkey within 3 months in 1999. Structures in many cities such as Duzce were affected by both earthquakes. The August 17 earthquake might have caused some damage earlier. The silos were located near a highway construction site within a very short distance from the fault line ruptured during the second earthquake, and 5 km away from the epicenter of that earthquake. The three identical liquefied gas storage tanks were located near the city of Izmit and were built in 1995.

During the 1999 Kocaeli earthquake, two of the three aboveground tanks collapsed as a result of failure of reinforced concrete columns supporting the tanks. The collapsed tanks contained liquefied oxygen and were 85% full, and the undamaged liquefied nitrogen tank was 25% full at the time of the earthquake. It is estimated that approximately 1200 metric tons of cryogenic liquefied oxygen were released as a result of collapse of the two oxygen storage tanks. The liquefied nitrogen tank next to the collapsed tanks was virtually undamaged. Based on the detailed dynamic analyses of the tanks, Sezen et al. (2008) [19] concluded that the sloshing of the stored fluid did not affect the tank response significantly, and the failure was mainly due to insufficient strength and deformation capacity of the columns supporting the oxygen tanks. They also concluded that if an elevated tank is desired in a seismic region, the strength and deformation capacity of the support columns should be increased considerably, or an alternative support structure should be used. Three reinforced concrete silos at the state-owned paper mill, SEKA, collapsed during the 1999 Kocaeli earthquake. The paper mill was located approximately 20 km from the epicenter of the earthquake. Fig. 15 shows photographs of two undamaged silos and a collapsed silo. The diameter of the silos was approximately 6 m. The collapsed silos were supported on six small square non-ductile columns with minimal longitudinal reinforcement. The undamaged silos of Fig. 16 were supported on larger square columns than those of the collapsed silos.

**September 21, 1999 Chi-Chi, Taiwan Earthquake**

An earthquake of occurred 7.6 magnitudes in Taiwan at 1:47 a.m. on September 21, 1999. A concrete factory silo fell to the ground during the earthquake. The upper portions of the collapsed silo suffered virtually no damage, suggesting that the integrity of the conical bottom segment and the anchorage to the foundation should be carefully considered during the seismic design of silos. Other silos that collapsed caused by the same earthquake were also reported. A report by EQE indicated that a food processing plant had several grain silos, which were filled with food products by the plant operators because of an impending typhoon predicted before the earthquake. When the earthquake hit, all of the full silos collapsed (EQE 1999) [7].

**May 21, 2003 Zemmouri, Algeria Earthquake**

An earthquake with a magnitude of 6.8 and a focal depth of 10 km occurred in the boundary region between the Eurasian plate and the African plate on May 21, 2003. At least 2,266 people were killed, and 10,261 injured (USGS 2003) [23]. The earthquake caused severe damage to some storage facilities and equipment. The spectacular damage to the Corso silos was mostly concentrated in the walls near the bottom of the silos. The silo complex was constructed during the 1970s near the city of Boumerdes. Five batteries compose the complex, which is founded on piles that are 24 m in length. Battery number five was the most damaged. At the time of the earthquake, the battery was nearly full with grain, whereas other batteries were either approximately half filled or almost empty. Severe concrete crushing, lack of sufficient reinforcement, steel bar fractures and buckling, and partial sliding of the external concrete shell were observed (Bechtoula and Ousalem 2005) [2].

**Cylinders under high internal pressure: elephant's foot**

Under high internal pressures, local collapse of the shell can occur. This is best known at a base boundary condition, where it has been often observed in tanks which have been subjected to earthquake loading, but it can also occur on the cylinder wall where a ring, thickness change or local imperfection occurs. The stress levels associated with this effect are considerably lower than the von Mises membrane yield envelope, as a result of the effect of amplified displacements near the disturbance. The first scientific study of this problem appears to have been that of Rotter, 1955 [18]. In that study, it was assumed that the local collapse and elastic buckling had little interaction, without proper justification. However, this has now been shown to be substantially true, by considering the local collapse at an axisymmetric weld depression. The strength at an "elephant's foot" failure at the boundary condition is somewhat lower than internal failures at local imperfections, but much more work is needed to establish a less conservative evaluation. The standard has adopted the approximate relationship

Methods of dealing with this type of failure (ECCS, 1988 [6], Bandyopadhyay et al., 1995[1]) involve complicated iterative calculations with no better foundation in rational mechanics. Where the shell is subjected to global bending, the ductility of this failure mode permits higher stresses to be achieved. The range of strength gains has been recently assessed and appears to lie in the range 30–50%, so further work on elephant's foot failures under combined axial compression and global bending would be useful.

**Modeling of granular materials:**

The proposed numerical model of the cylindrical r.c. silo bin system consists of three types of finite elements (see Fig.1):

- reinforced concrete silo bin wall elements,

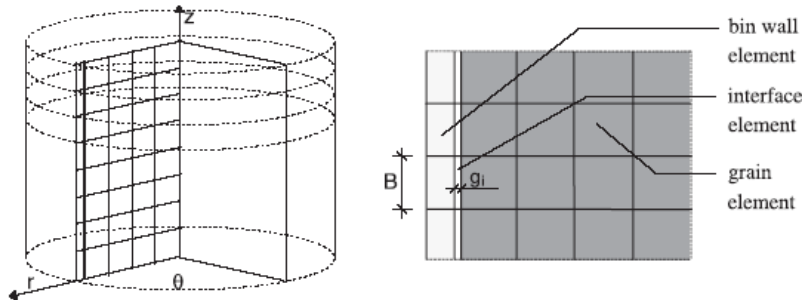


**Fig. 1.** Conception of numerical discretisation of axi-symmetric silo wall-bulk solid system.

- Hypothetical contact layer (interface layer),
- Bulk solids elements.

The following assumptions were formulated for the first numerical FEM model taking into account the imposed actions coupled with permanent bulk solid pressure (Gnatowski, 1998) [8]:

- The FEM analysis was applied to the cylindrical r.c. wall structure (considered here as a thin cylindrical shell),
- Constant distribution of imposed action on the silo wall over the wall perimeter,
- Granular, non-cohesive particulate solid,
- The computational model based on real behaviour of bulk solid with application of the nonlinear elastic theory,
- The reinforced concrete silo wall described by constitutive laws of elastic linear theory of the cylindrical shell.

To describe the phenomena taking place on the surface between the granular medium and the silo wall, an adaptation of a thin contact layer (interface element) proposed by Desai et al., 1986 [4] is applied. The following matrix has been used in the formulation of the problem:

$$[D]_i = \begin{bmatrix} d_1 & d_2 & d_2 & 0 \\ & d_1 & d_2 & 0 \\ & & d_1 & 0 \\ \text{SYM} & & & G_i \end{bmatrix} \quad \text{Matrix (1)}$$

and:

$$d_1 = \lambda_2 [E_m (1 - \nu_m)] / [(1 + \nu_m)(1 - 2\nu_m)],$$

$$d_2 = \lambda_2 [E_m \nu_m] / [(1 + \nu_m)(1 - 2\nu_m)],$$

$$\lambda_2 = 1.0$$

Where:  $E_m$  and  $\nu_m$  are the modulus of elasticity and Poisson's ratio of bulk solid, respectively.

To define shear modulus  $G_i$  given in matrix (1) an empirical relationship between shear stresses  $\tau_s$  and relative displacement  $s$  at the contact zone should be obtained experimentally from direct shear apparatus tests. On the above basis, the following formula has been used:

where:  $n$  experimental parameters,  $L$  displacement modulus [mm],  $\mu$  the coefficient of friction of bulk solid at the contact surface,  $\sigma_n$  stress in normal direction to the contact surface,  $\tau_{s,max}$  maximum value of shear stress. The experimental relationship obtained here in the formulation

(For wheat) in the direct shear apparatus is presented in Fig. 2.

Taking into account  $\gamma = s/g_i$  and  $G_i = d\tau_s/d\gamma$  the following formula was obtained

$$G_i = \frac{d\tau_s}{d\gamma} = n \frac{g_i}{L} \mu \sigma_n \left( \frac{L}{g_i \gamma} \right)^{(n-1)} \exp \left( - \frac{g_i \gamma}{L} \right)^n$$

The experimental relationship obtained here in the formulation (for wheat) in the direct shear apparatus is presented in Fig. 2 (Lapko et al. 2003)[25].

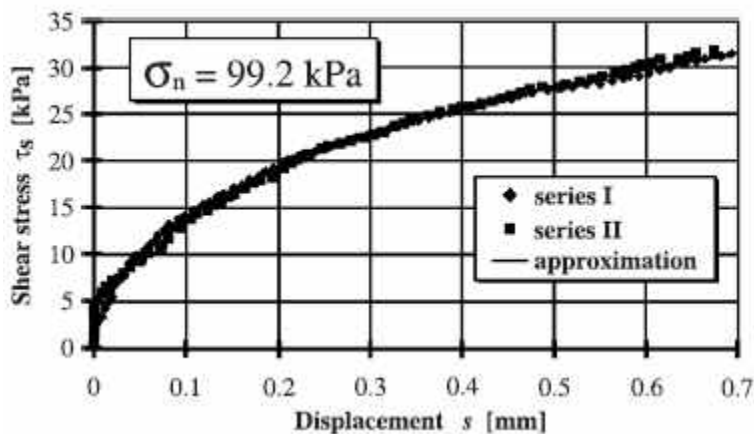


**Fig. 2.** Experimental curves obtained from direct shear apparatus tests for wheat considered in the FEM model description.

For the needs of numerical analysis of the interaction effects between silo wall structure and bulk solid, the nonlinear approach proposed by Duncan and Chang, 1970 [5] has been here adopted. The stiffness matrix of the finite element modelling the mass of bulk solid is used in the following way:

$$[D]_m = \begin{bmatrix} d_{11} & d_{12} & d_{13} & 0 \\ & d_{22} & d_{23} & 0 \\ & & d_{33} & 0 \\ SYM & & & G_m \end{bmatrix}$$

Where the components of the matrix are denoted as follows:

$$d_{11} = d_{22} = d_{33} = \frac{E_m(1-\nu_m)}{(1+\nu_m)(1-2\nu_m)}$$

$$d_{12} = d_{13} = d_{23} = \frac{E_m\nu_m}{(1+\nu_m)(1-2\nu_m)}$$

$$G_m = \frac{E_m}{2(1+\nu_m)}$$

In order to determine the modulus of elasticity  $E_m$  of bulk solid, the numerical iterations procedures proposed by Duncan and Chang [5] were applied:

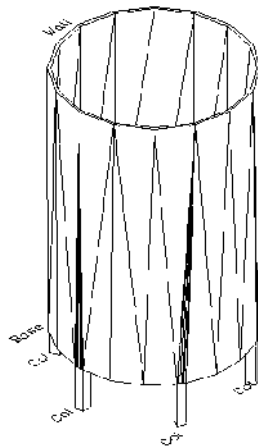
$$E_m = \left[ 1 - \frac{Q_f(1-\sin\phi)(\sigma_1 - \sigma_3)}{2c\cos\phi + 2\sigma_3\sin\phi} \right]^2 KP_a \left( \frac{\sigma_3}{P_a} \right)^m$$

Where:  $\sigma_1$  and  $\sigma_3$  principal stresses (max. and min.),  $c$  cohesion of bulk solids,  $\phi$  internal friction angle,  $K$  and  $m$  material parameters,  $P_a$  value of atmospheric pressure,  $Q_f$  experimental coefficient. This assumptions and relationships were elaborated with the use of the iteration algorithm and then applied in a computer program Gnatowski, 1998 [8]. In the general issues concerning the actions provoked by earthquake ground motion on the walls of flat-bottom grain silos, the assessment of the horizontal actions seems to be of particular interest. These actions are usually evaluated under the following hypotheses:

- (i). Stiff behaviour of the silo and its contents (which means considering the silo and its contents to be subjected to ground accelerations);
- (ii). The grain mass corresponding to the whole content of the silo except the base cone with an inclination equal to the internal friction angle of the grain is balanced by the horizontal actions provided by the walls (supposing that the seismic force coming from the base cone is balanced by friction and therefore does not push against the walls).

This design approach is not supported by specific scientific studies; as a matter of fact, even though there are many papers on the behaviour of liquid silos under earthquake ground motion (Hamdan 2000 [9], Nachtigall 2003 [16]), there are no examples of scientific investigation into the dynamic behaviour, let alone under earthquake ground motion, of flat-bottom grain silos.

The main goal of the paper is to present analytical developments devoted to the evaluation of the effective behaviour of flat-bottom silos containing grain, as subjected to constant horizontal acceleration and constant vertical acceleration. In more detail, the developments presented here, keeping the validity of the hypothesis (i), aim to assess the effective horizontal actions that rise on the silo walls due to the accelerations, by means of analytical studies and on the basis of dynamic equilibrium considerations.

**Fig. 3. Silo Model**

The analyses reported here are developed by simulating the earthquake ground motion with constant vertical and horizontal accelerations (time-history dynamic analyses are not carried out). The results obtained show how these horizontal actions are far lower with respect to those that can be obtained using the hypothesis (ii).

To better understand the physical meaning of the results obtained a physical representation of the results in terms of portions of grain mass which actually weigh (in terms of horizontal actions) upon the silo walls is also provided, in addition to the analytical expression of the horizontal actions. The results obtained are then used to formulate a procedure for the seismic design of silos.

## 2. Modeling the Silos

Seven finite element models of the present work were used to analyze different cylindrical silos with flat bottom. The following table 1 was the dimensions of the silos:

**Table 1.**

Dimension of the examined silos

Diameter	D	5	5	5	10	10	20	20
Height	H	16	20	30	16	30	16	60
Ratio	H/D	3.2	4	6	1.6	3	0.8	3
Models		(1)	(2)	(3)	(4)	(5)	(6)	(7)

**Tale 2.**

Dimension of silos Models

Models	(1)	(2)	(3)	(4)	(5)	(6)	(7)
column Size	50x50	50x50	55x55	50x50	70x70	50x50	100x100
Wall thickness	25	25	30	25	30	25	35
Base thickness	40	40	45	40	45	40	50

### 2.1. Finite element model

For the finite element modeling, we used five of the element types available in the SAP2000, and to simulate the stored material we used interface elements Solid (Fig. 1). Since FEM is a continuum method, one must use a constitutive law capable of approximating the behaviour of a granular material consisting of discrete particles.

### 2.3. Static conditions

It is known that the grain provides a vertical push onto the silo walls. It can be hypothesized that the vertical pressures actually tend to diminish from the core of the grain portion until they disappear when the grain meets the silo walls. A limiting schematization (that will be useful for the assessment, to guarantee safety, of the actions induced on the silo walls by the vertical accelerations, as illustrated in the following sections) is one where the grain is divided into two “equivalent” portions composed of (i) grain completely leaning against the layers below (central portion) and (ii) grain completely sustained by the walls (and therefore characterized by a null vertical pressure between one grain and another).

It has been argued that a better understanding of the properties of the ensiled materials and their interaction with the silo structure is one of the critical factors in improving design. (Johnston, 1981) [11].

The behavior of the granular element was described with a micro-polar hypoplastic constitutive model [(Tejchman and Gudehus, 2001) [20], (Tejchman and Górski, 2008) [21], (Tejchman et al., 2008) [22] which takes into account the evolution of effective stresses and couple stresses depending on the current void ratio, stress and couple stress state, rate of deformation and rate of curvature and a mean grain diameter. The feature of this model is a simple formulation and procedure for determining the material parameters with standard laboratory experiments (Herle and Gudehus, 1999) [10]. The material parameters are related to the granulometric properties of granular materials, such as grain size distribution curve, shape, angularity and hardness of grains. The model is capable to describe a transition between dilatancy and contractancy during shearing with constant pressure and a transition between an increase and a decrease of pressure during shearing with constant volume. The finite element results are mesh-insensitive during boundary value problems involving shear localization due to the presence of a characteristic length in the form of a mean grain diameter (McKee et al., 1995) [13].

### 4.1. Static and dynamic wall pressure

The Janssen's formula (Janssen 1895) [26] is used to predict the wall pressure of silos can be written as:

$$P = \frac{\gamma \cdot r}{\mu} \cdot k; k = \left[ 1 - e^{\frac{h}{h_0}} \right], r = \frac{A}{O} = \frac{\text{Area}}{\text{Parameter}}, h_0 = \frac{r}{\lambda \cdot \mu}$$

; ( $\phi_{\text{filling}} = 0.75\phi$ ,  $\phi_{\text{Emptying}} = 0.6\phi$ ),  $\mu = \tan \phi$  (coefficient of friction between wall and the bulk material) ( $\mu_f = \tan \phi_{\text{filling}}$  for filling case,  $\mu_e = \tan \phi_{\text{emptying}}$  for emptying case).

The static design of silos is usually done in accordance with the established physical idealization suggested by Janssen (26). Fig. 4 shows the pressure against silo wall during filling and discharging recommended by different codes.

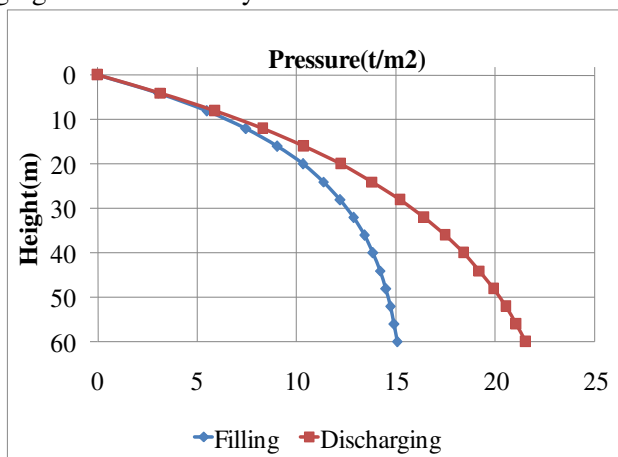


**Fig. 4.** Filling and Discharging Pressure according to Codes

Table 3 shows the parameters used in this paper for both static and dynamic analysis of the different kinds of silos.

**Table 3.**

Mechanical properties of Spanish Horzal wheat (Vidala et al., 2008) [24]

Property	Value
Specific Weight ( $\gamma$ ) (KN/m <sup>3</sup> )	8.4
Young's modulus (E) (KPa)	5129
Poisson's ratio ( $\nu$ )	0.32
Grain-wall friction coefficient	0.2
Internal friction angle ( $\phi$ ) (°)	25
Apparent cohesion (c) (KPa)	3
Dilatancy angle (°)	17.6

A 3D finite-element model shown in figure 1 was developed to study pressures on the large diameter silo wall used FEM software SAP2000 [3]. The element used to represent the stored material was 3D solid element, a cubic element defined by eight nodes with three degrees of freedom and a nodal displacement at x, y, and z. This structural element is compatible with surface-to-surface contact elements that admit different plasticity models and laws of behavior of the bulk material. This study simulates silos filled with wheat, a granular material that can be reasonably considered isotropic, particularly when it is randomly packed. Because wheat is a granular material, a law of behavior of the stored material must be used that reproduces the behavior of wheat grains with low cohesion. In this study, the bulk solid was simulated by Mohr-Coulomb model which was based on a non-associated flow rule, a perfectly-plastic Mohr-Coulomb yield behavior and tension

cut-off. The Mohr-Coulomb yield equation can be written as  $f = \alpha I_1 + \sqrt{J_2} - k$ , where  $\alpha$  and  $k$  are stressed dependent:

$$\alpha = \frac{2 \sin \phi}{3(1 - \sin \phi) \sin \theta + \sqrt{3}(3 + \sin \phi) \cos \theta}, \quad k = \frac{6c \sin \phi}{3(1 - \sin \phi) \sin \theta + \sqrt{3}(3 + \sin \phi) \cos \theta},$$

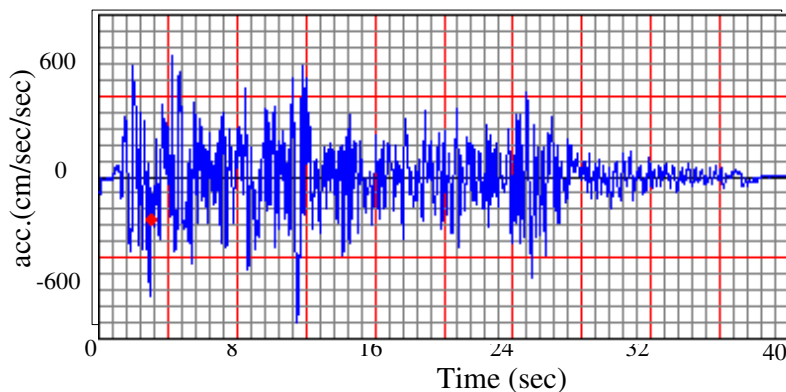
$$\theta = \frac{1}{3} \cos^{-1} \left( \frac{3\sqrt{3}}{2} \frac{J_3}{J_2^{3/2}} \right)$$

$I_1$  is the first stress invariant at time  $t$ ,  $J_2$  is the second deviatoric stress invariant at time  $t$ ,  $J_3$  is the third deviatoric stress invariant at time  $t$ .  $\phi$  is the friction angle (a material constant),  $c$  is the cohesion (a material constant). Although, more complex models exist, the Mohr-Coulomb model is sufficiently accurate and easy to use with numerical models.

A surface-to-surface contact model was used between the bulk solid and silo wall. Two surfaces that contactor surface and target surface made up a contact pair. The contactor surface was the out surface of bulk solid and the target surface was silo wall. Because the Young's modulus of reinforcement concrete is about 20 GPa, which is much larger than the Young's modulus of stored material, the silo wall was considered to be rigid for good convergence in this paper.

#### Input loading:

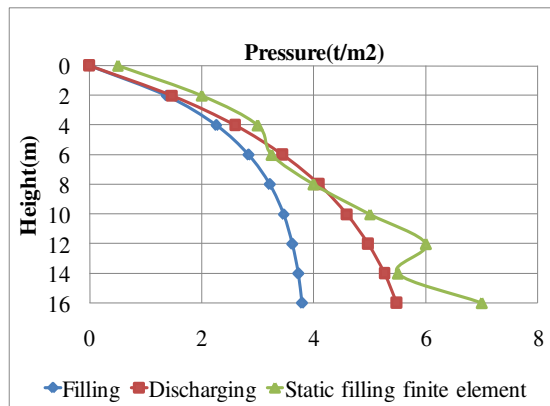
The dynamic analysis of the different kinds of silos will establish by time history analysis using Elcentro earthquake model (as shown in Fig. 5) as 0.5g of the ground acceleration.



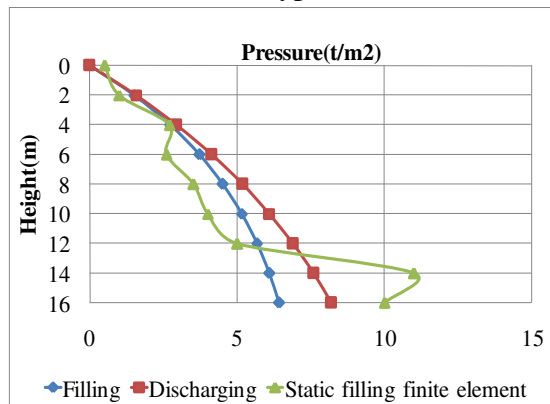
**Fig. 5. El Centrio Model Vibration**

Figure 6 shows the comparison between filling, discharging pressures and finite element analysis when the silo is full of wheat. As illustrated from Fig. 6, the discharging pressures envelope the finite element pressures as the silo is full in the upper half of silo height except in the lower of the silo the finite element pressures envelope the recommended pressures during discharging. Fig. (6) Illustrated that the result of finite element ( $h/d = 1 - 2$ ) the pressure in squat silos curve come closest to the straight line. For wheat silos with great aspect ratio the peak filling pressure as the silo is full equals two times that is determined analytically from Janssen equation. However, in case of large silos

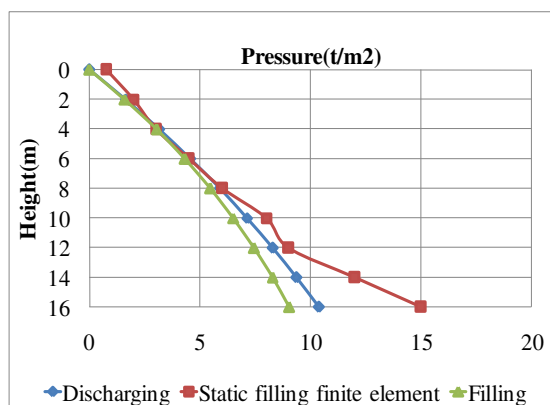
with small aspect ratio the peak filling pressure due to finite element is about 1.6 times the discharging pressure determined according to Janssen equation.



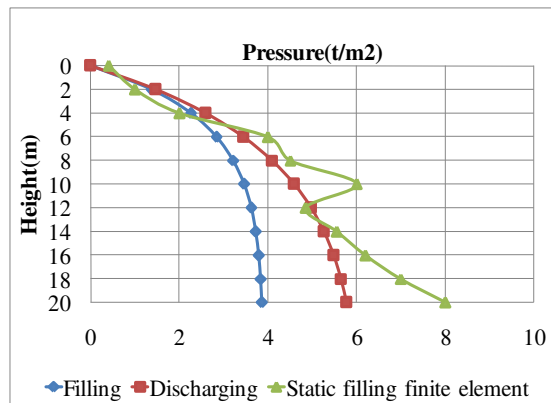
i) Silo type (model 1)



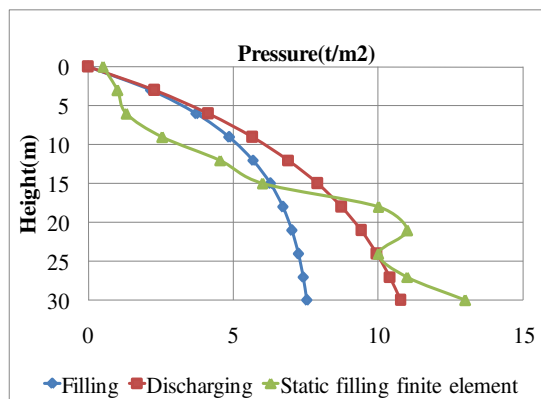
ii) Silo type (model 4)



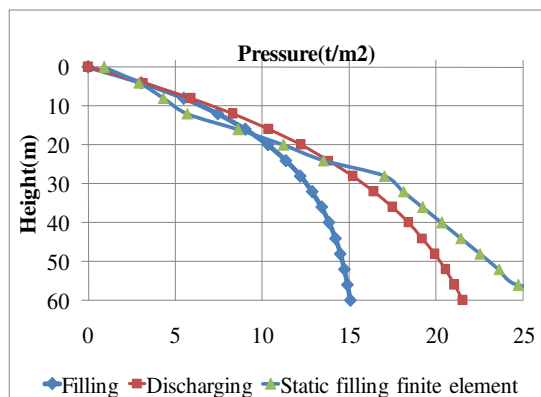
ii) Silo type (model 6)



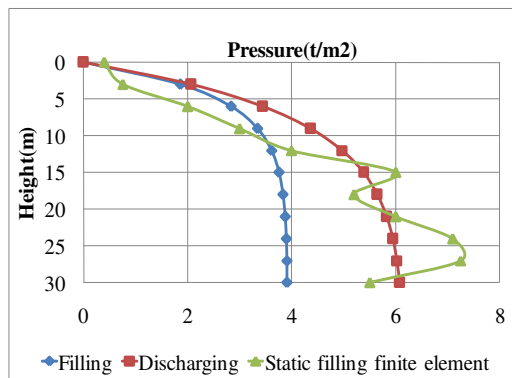
iv) Silo type (model 2)



v) Silo type (model 5)



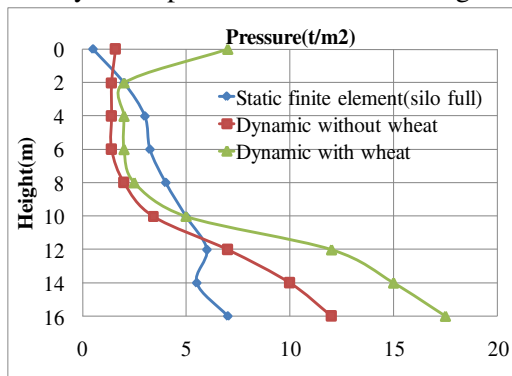
vi) Silo type (model 7)



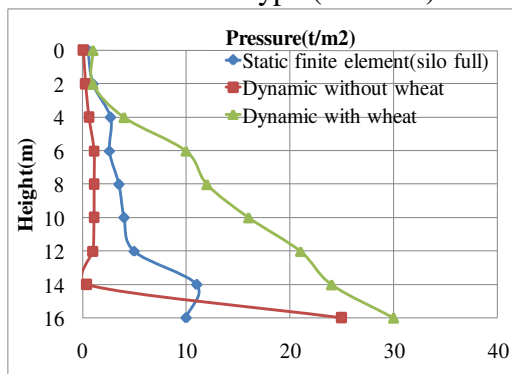
vii) Silo type (model 3)

**Fig. 6.** Comparison between recommended filling and discharging pressures in different silo types with finite element pressures as the silo is full

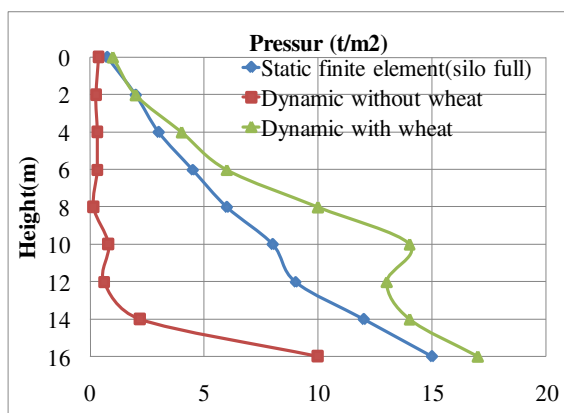
Figure 7 illustrates the comparison between pressures in static and dynamic cases. All types of silos show a rise in dynamic pressure values at all heights



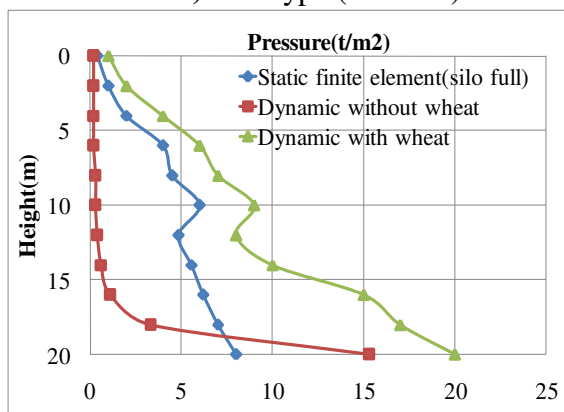
i. Silo type (model 1)



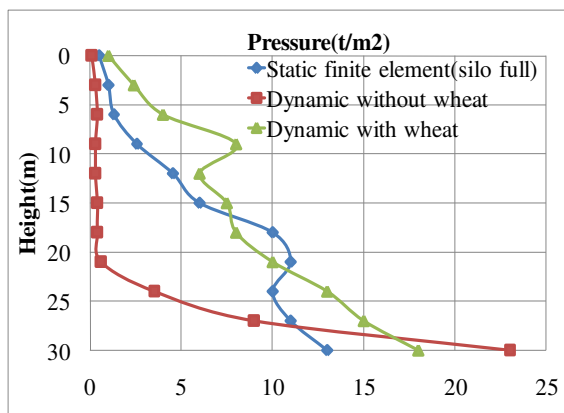
ii) Silo type (model 4)



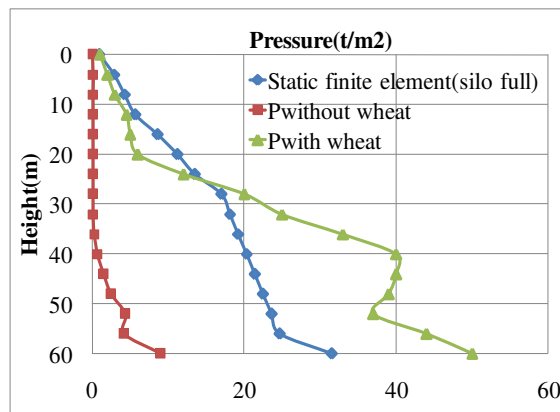
iii) Silo type (model 6)



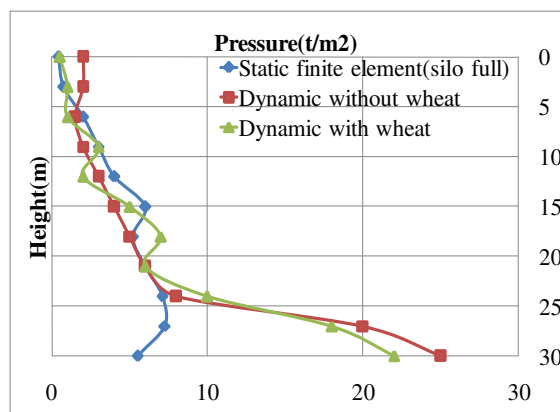
iv) Silo type (model 2)



v) Silo type (model 5)



vi) Silo type (model 7)



vii) Silo type (model 3)

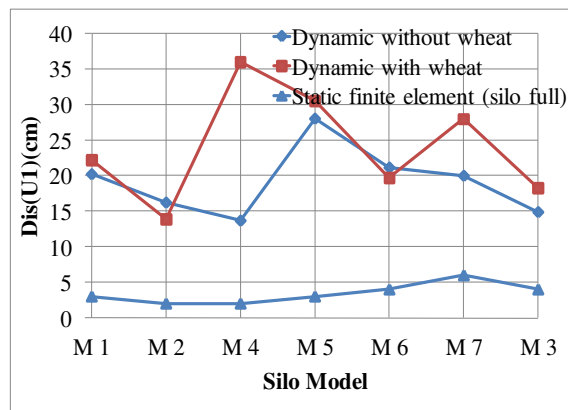
**Fig. 7.** Comparison between the obtained finite element static and dynamic pressures in different silos types

Fig. 7 ( $h/d = 16/5-16/10-16/20$ ) illustrate the finite element filling and dynamic pressures as the silo diameters varies from 5-10-20 m. while the silo height is constant (16.0 m). In these models (Large diameter silos), The dynamic pressure values envelope the finite element filling pressure in the all points especially in the lower half of the silo height. However by increasing ( $h/d$ ) ratio the filling pressure values envelope the dynamic pressure values in the upper half of silo height. This means that in large diameter silos ( $h/d = 1-2$ ). The vibration of granular material inside the silo part situated near the top surface plays an important role in these silos responses.

Fig.7 (i,iv,vii), (ii,v),(iii,vi) exhibits the compression of the dynamic and static pressure as the silo is full with constant diameter the height from ( 16m – 20m – 30m – 60m ) and for different  $h/d$  ratios = (3-4-5),(1.6-3) and (0.8-3) respectively. As shown in these figures, the dynamic pressure is equal to (3-5) ; (1.5 -3) and (1.6-2) times the filling pressures

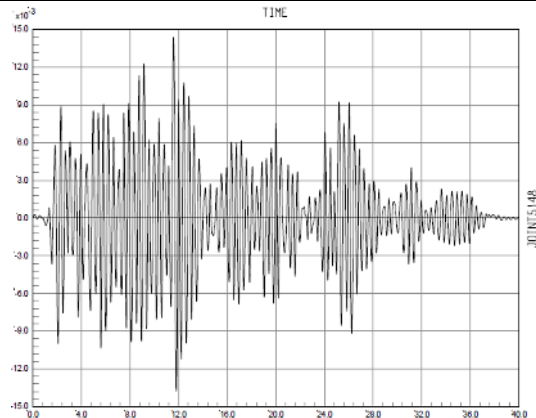
respectively. In the squat (Large diameter silos), the max dynamic pressure occurs at 0.65 H from the silo top and equals 2 times the filling pressure.

Figure (8) shows the comparison between deformations in X direction in different silos types. As shown in figure (8) the values of displacement in X direction in static (both cases empty and full cases) are negligible values with respect to the values of displacements in dynamic cases (both empty and full cases). The arrangements from high to low dynamic deformations for both cases full and empty are M7, M1, M2, M5, M6, M4 short, and m. The ratios between deformations in full and empty cases are 3.56, 6.19, 5.91, 9.55, 12.28, and 13.94. The high values of deformation for full silos under dynamic load (earthquake) related to the sloshing effect of the bulk solid in the different cases of silos so, its X direction deformation is multiplication specially M7, and M4 cases.

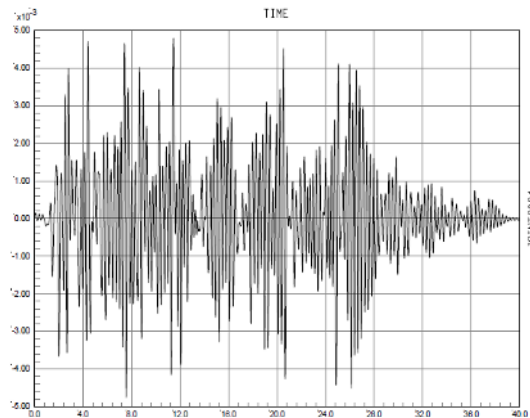


**Fig. 8.** Comparison between deformations in X direction in different silos models

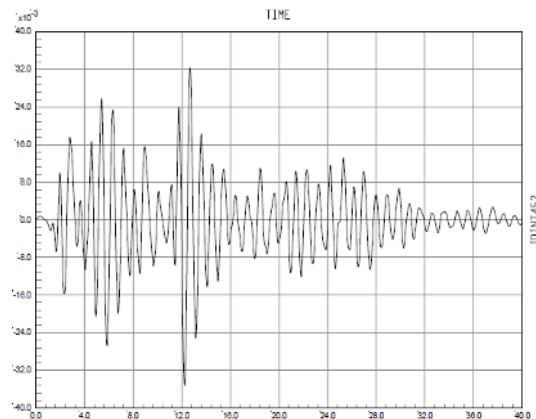
Figure 9 shows time history of displacement of top point of the different types of diameter height ratios of silos. The silo top displacement time history provides pronounced significant responses due to strongly variation of displacement impulsations in the squat silos of small height and large diameter with ratio ( $h/d = 1 - 2$ ) while, in tall silos having the same diameter the seismic load cause the extreme top displacement with small and quiet fluctuations due to the large mass of ensiled materials in tall silos.



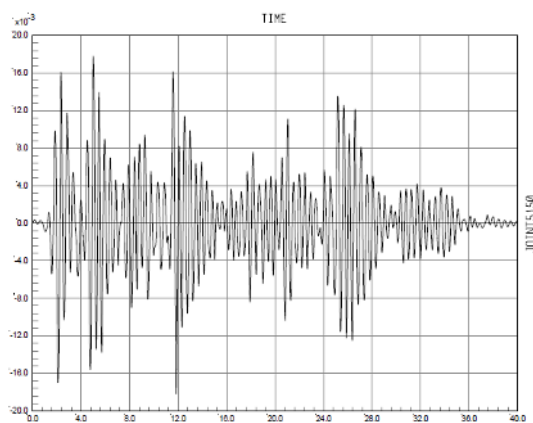
**i) Silo type (model 1)**



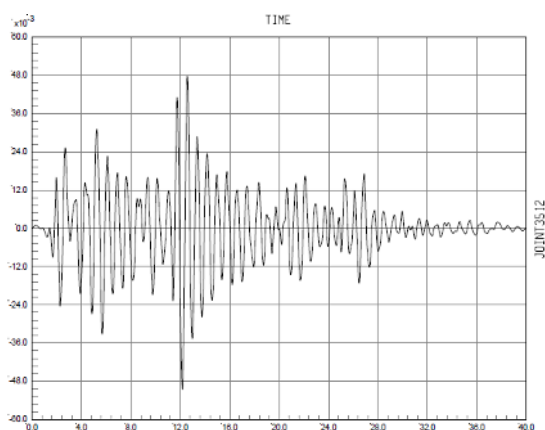
**ii) Silo type (model 4)**



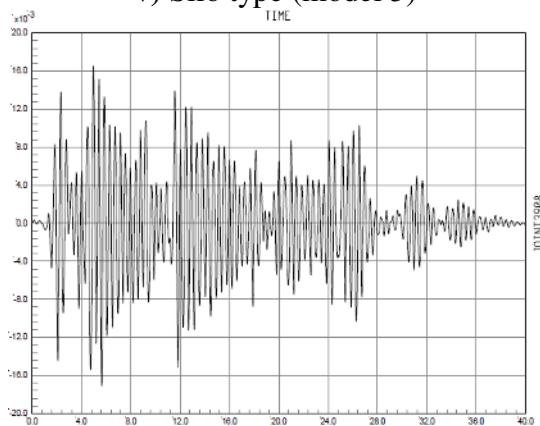
**iii) Silo type (model 6)**



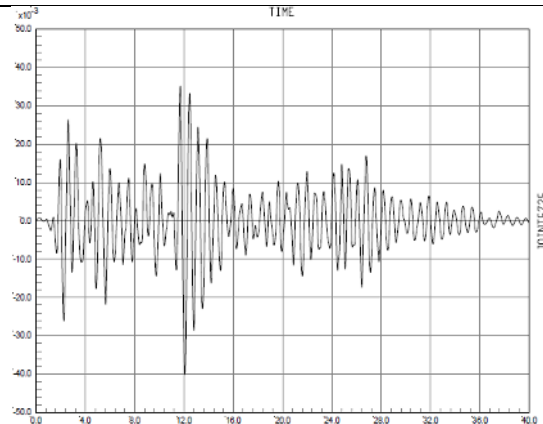
**iv) Silo type (model 2)**



**v) Silo type (model 5)**



**vi) Silo type (model 7)**

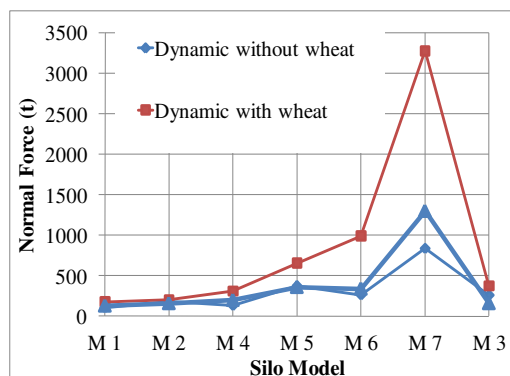
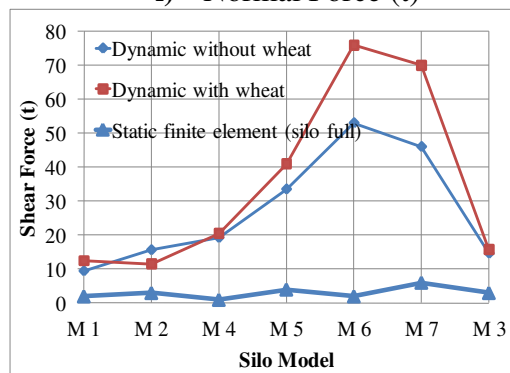


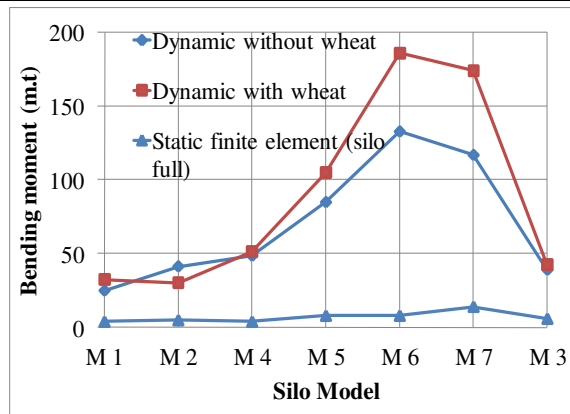
vii) Silo type (model 3)

**Fig. 9.** Time History of displacement in X-direction of Silos of different diameter height ratios

(Displacement in m)

Figure 10 shows the straining action on columns support silos models under dynamic effect in cases of empty and full cases under earthquake.

**i) Normal Force (t)****ii) Shear force (t)**



iii) Bending Moment (m.t.)

**Fig. 10.** Straining action on columns support silo models

From Fig. 10 it is observed that the normal forces on elevated wheat silo supports is significantly increased especially in the large diameter silos with large height due to the large material stacked up very high vertically. The included normal force in the support column due to vibration of the ensiled material in such silos is equal to 2.4 times that induced as the silo is full only. In small diameter silos the normal force ratio in case of with and without the ground motion is equal 1-2 i.e., the effectiveness of seismic ensiled material on the support normal forces increases with the increase of material mass.

## 5. Conclusions

This paper offers a review and more understanding of available technique information with regards of behavior of wheat silos under seismic load. In this paper a 7 RC wheat silos with different height to diameter ratios has been utilized and subjected to earthquake records considering the ensiling materials. The dynamic analysis concludes that the seismic response of silos is significantly affected by earthquake characteristics. The following conclusion can be drawn from the foregoing presentation and discussion:

- The effect of the ground motion on the silos taking into the account the ensiling material has highly influence by the earthquake characteristic. In particular, it is found that the ensiling material may increase maximum pressure by 3 – 5 times the FE filling pressure in tall silos ( $h/d = 3 - 6$ ). The maximum pressure occurs at the silo base.
- In silos characterized by squat geometrical configuration ( $h/d = 1 - 2$ ) and in large diameter silo, vibration of ensiled material increases the silo wall pressure by two times the FE filling pressure without earthquake. The maximum occur at  $0.65h$  from the silo top.
- The silo top displacement time history provides pronounced significant responses due to strongly variation of displacement impulsations in the squat silos of small height and large diameter with ratio ( $h/d = 1 - 2$ ) while, in tall silos having the same diameter the seismic load cause the extreme top displacement with small and quiet fluctuations due to the large mass of ensiled materials in tall silos.

- The pressure increase due to the ensiled wheat during the ground motion is considerable larger than that recommended discharging pressure resulting from multiply Janssen equations by some factors. Consequently these dynamic pressures appear due to the ensiled materials govern the practical design of those silos.
- The actions provoked by the earthquake ground motion on the ensiled material lead to remarkable increase in the normal, shear forces and bending moments on the supports the effect of ensiled material turns out to be noticeably in large diameter silos.
- The effect of ensiled material in silos during the ground motions deserve more attention and should be included in the future versions of seismic codes.

## 6. References

- [1] Bandyopadhyay K, Cornell A, Costantino C, Kennedy R, Miller C, Veletsos A. Seismic design and evaluation guidelines for the Department of Energy high-level waste storage tanks and appurtenances. Department of Advanced Technology, Brookhaven National Laboratory, Associated Universities, October 1995.
- [2] Bechtoula, H., and Ousalem, H. (2005). "The 21 May 2003 Zemmouri (Algeria) earthquake damages and disaster responses." *J. Adv. Concr. Technol.*, 3(1), 161–174.
- [3] CSI, 2005. *SAP2000: Static and Dynamic Finite Element Analysis of Structures*, Advanced9.1.4, Computers and Structures, Inc., Berkeley, California.
- [4] C.S. Desai, M.M. Zaman, J.G. Lightner, H.J. Siriwardane, Thin-layer element for interfaces and joints, *International Journal for Numerical and Analytical Methods in Geomechanics* 8 (1984) 19–43.
- [5] J.M. Duncan, C.Y. Chang, Nonlinear analysis of stress and strain in soils, *Journal of the Soil Mechanics and Foundations Division, Proceedings of the ASCE* 96 (SM5) (1970 September).
- [6] ECCS. European recommendations for steel construction: buckling of shells, 4th ed. Brussels: European Convention for Constructional Steelwork, 1988.
- [7] EQE. (1999). "Chichi, Taiwan earthquake of September 21, 1999 (M7.6)." An EQE Briefing, ([http://www.absconsulting.com/resources/ Catastrophe \(Reports/Chichi-Taiwan-1999.pdf\)](http://www.absconsulting.com/resources/Catastrophe%20Reports/Chichi-Taiwan-1999.pdf)) (Jan. 29, 2008).
- [8] M. Gnatowski, Statical analysis of r.c. concentric silo bins taking into account the interaction between wall structure and bulk solids, PhD thesis, Bialystok, 1998, in Polish.
- [9] Hamdan, F.H. 2000. Seismic behaviour of cylindrical steel liquid storage tanks, *Journal of constructional Steel Research*, Vol. 53, p. 307–333.
- [10] I. Herle, G. Gudehus, Determination of parameters of a hypoplastic constitutive model from properties of grain assemblies, *Mechanics of Cohesive-Frictional Materials* 4 (5) (1999) 461–486.
- [11] Johnston, F. T. Silo problems. In *Proc. 6th Powder and Bulk solids Con\$, Rosemont, Illinois, 1981*, pp 97-102
- [12] Li, H. (1994). "Analysis of steel silo structures on discrete supports." Ph.D. thesis, Univ. of Edinburgh, Edinburgh, Scotland, U.K.
- [13] S.L. McKee, T. Dyakowski, R.A. Williams, T.A. Bell, T. Allen, Solids flow imaging and attrition studies in a pneumatic conveyor, *Powder Technology* 82 (1995) 105–113.
- [14] Mendez, D. \_2001\_. "Stunned Salvador suffers second deadly quake in a month." *The BG News*, Feb. 14, <http://media.www.bgnews.com/media/storage/paper883/news/2001/02/14/World/Stunned.Salvador.Suffers.Second.Deadly.Quake.In.A.Month-1283510.shtml>\_ \_Jan. 22, 2008\_.

- [15] Moran, D., Ferver, G., Thiel, C., Stratta, J., Valera, J., and Whyllie, L. \_1975\_. "Lima, Peru Earthquake of October 1974." A Reconnaissance Rep.,
- [16] Nachtigall, I., Gebbeken, N., Urrutia-Galicia, J.L. 2003. *On the analysis of vertical circular cylindrical tanks under earthquake excitation at its base*. Engineering Structures, Vol. 25, p. 201–213.
- [17] National Geophysical Data Center \_NGDC\_. \_1998\_. "Earthquake damage, the Armenian SSR, December 7, 1988." NGDC Natural Hazards Slide Set Thumbnails Header, [http://www.ngdc.noaa.gov/nndc/struts/results?eq\\_1\\_11&t\\_101634&s\\_0&d\\_2d&\\_22\\_Jan.26,2008\\_](http://www.ngdc.noaa.gov/nndc/struts/results?eq_1_11&t_101634&s_0&d_2d&_22_Jan.26,2008_).
- [18] Rotter JM. Local inelastic collapse of pressurised thin cylindrical steel shells under axial compression. Journal of Structural Engineering, ASCE 1990;116(7):1955–70.
- [19] Sezen, H., Livaoglu, R., and Dogangun, A. \_2008\_. "Dynamic analysis and seismic performance evaluation of above-ground liquid containing tanks." Eng. Struct., 30\_3\_, 794–803.
- [20] J. Tejchman, G. Gudehus, Shearing of a narrow granular strip with polar quantities, International Journal for Numerical and Analytical Methods in Geomechanics 25 (2001) 1–28.
- [21] J. Tejchman, J. Górski, Computations of size effects in granular bodies within micro-polar hypoplasticity during plane strain compression, International Journal of Solids and Structures 45 (6) (2008) 1546–1569.
- [22] J. Tejchman, W. Wu, R. Borja (Eds.), FE modeling of shear localization in granular bodies with micro-polar hypoplasticity, Springer, 2008.
- [http://www.eeri.org/lfe/pdf/peru\\_lima\\_eeri\\_preliminary\\_reconnaissance.pdf](http://www.eeri.org/lfe/pdf/peru_lima_eeri_preliminary_reconnaissance.pdf)\_Jan. 26, 2008\_.
- [23] USGS. \_2003\_. "Historic earthquakes, magnitude 6.8 Northern Algeria." [http://neic.usgs.gov/neis/eq\\_depot/2003/eq\\_030521/](http://neic.usgs.gov/neis/eq_depot/2003/eq_030521/)\_Jan. 27, 2008\_.
- [24] P. Vidala, E. Gallegob, M. Guaitac, F. Ayugad. "Finite element analysis under different boundary conditions of the filling of cylindrical steel silos having an eccentric hopper", Journal of Constructional Steel Research 64 (2008) 480–492.
- [25] A. Lapko, M. Gnatowski, and J.A. Prusiel "Analysis of some effects caused by interaction between bulk solid and r.c. silo wall structure" Powder Technology 133 (2003) 44– 53.
- [26] Janssen, H.A. 1895. Versuche uber Getreidedruck in Silozellen. Z. Vereines Deutscher Ingenieure 39:1045-1049.

## استجابة صوامع تخزين القمح المرفوعة للأحمال الزلزالية

### الملخص العربي

ترجع أهمية صوامع الخرسانية الاسطوانية إلى استخدامها في تخزين المواد الحيوية وهي حبل الحياه وتعتبر استراتيجية مهمة جدا بسبب استخدامها بشكل حيوي في الصناعات. ويعتبر ضغط مواد التخزين على حوائط التخزين للصوامع هو الدليل الوحيد لتصميم المنشآت الصومعية وان الضغط على الحوائط يزداد في حالة تفريغ الصومعة عن الضغط الاستاتيكي وهي مملوءة.

لذلك تعتبر صوامع التخزين من المنشآت الخاصة التي تتعرض للانهيارات الغير عادية نتيجة لتعرضها لاحمال متعددة و غير مالوفة بالاضافة الى ان الصوامع المرفوعة تختلف في السلوك الانشائي عن الصوامع على الارض عند تعرضها للهزات الارضي نظرا لتعرض مائة التخزين للهزات الارضية لذلك تعمل على زيادة جوهريه للضغط على حوائط الصوامع و قد يؤدي تعثر هذه المنشآت من خلال حركة الارض القوية الى احداث خطيرة. لهذا يهدف هذا البحث الى تقييم و تقديم الزيادة في الضغوط على الحوائط الصوامع المرفوعة اخذا في الاعتبار وجود مادة التخزين و مقارنة هذه الضغوط بنظيرتها الاستاتيكية الناجمة عن

التحليل الانشائي وكذلك بالضغط المحسوبة بالنظريات الحسابية في حالة الملا والتفريغ. تم اخذ التداخل و التوصل المقترح بواسطة ديساي (4) لتمثيل التأثير المفروض والموصول بمادة التخزين على حوائط الصوامع اثناء الهزات الارضية. وقد اختير البحث اللاخطي المقترح بواسطة دونكن و شانج(5). لتمثيل اللاخطية لمادة التخزين لحساب المعاملات التكرارية الناجم عن التشكلات الجديدة و المتخلفة اثناء الحركات الارضية وكذلك اخذ علاقة التبعية للانفعال و الاجهاد طبقا لى لايكوا(25). وفي هذا البحث تمت دراسة و تحليل عدد 7 نموذج من الصوامع الاسطوانية الخرسانية المختلفة في نسبة الارتفاع الى القطر تحت تأثير زلزال افقى من سجلات الزلازل بعجلة مقدارها 0.50 عجلة الجاذبية باستخدام تقنية نمودجية ميكانيكية محدودة العنصر .

وقد اظهرت النتائج ما يلي :

- في الصوامع شاهقة الارتفاع لوحظ ان الضغط على حوائط الصوامع يزداد بصورة جوهرية ويتراوح من 3-5 مرات الضغط الاستاتيكي على حوائط الصوامع معتمدا على نسبة العمق الى القطر .
- في الصوامع القرفصائية التي لها نسبة العمق الى القطر (1-2) يزداد الضغط على حوائط الصوامع بمقدار (1-2) مرات الضغط الاستاتيكي بدون اعتبار الهزات الارضية .
- في الصوامع القرفصائية ذات العمق الى القطر (1-2) و ذات الاقطار الكبيرة تتعرض نبضات الازاحة العلوية لتغيرات و تمايلات قوية متتابعة بينما في الصوامع الطويلة بنفس القطر تسبب الاحمال الزلزالية ازاحة اقل نسبيا و تمايلات هادئة في النبضات نتيجة و جود مادة التخزين اثناء الهزات الارضية .
- زيادة الضغط على الحوائط نتيجة احتواء مادة التخزين اثناء الهزات الارضية اكبر بكثير عن الضغط الناتج من تفريغ هذه الصوامع والمذكى بمعظم بلدان العالم بضرب معادلة يانسن (26) في معامل لكل مادة من مواد التخزين ويتضح من هذه النتائج ان هذا التأثير يتحكم في تصميم هذه الصوامع .
- الاداء او التصرف المستقر للهزات الارضية للصوامع المملوءة بمادة التخزين يقود إلى زيادة كبيرة في القوى الرأسية و قوى القص و عزوم الانحناءات في الركائز الحاملة للصومعة يجعلها جديرة في الاعتبار عند تصميم هذه المنشآت.
- إحتواء التأثير المتبادل لمادة التخزين داخل الصوامع اثناء الهزات الارضية يستحق اهتمام أكثر ويجب إحتوائها و أخذها في الاعتبار في نص نسخ الكود لاحمال الزلازل في المستقبل .